Frequency Beamforming-Enhanced DBIM for Limited-Aperture Quantitative Imaging

Scott Ziegler and Matthew Burfeindt
U.S. Naval Research Laboratory, Washington, D.C., 20375, USA

***Abstract*—The distorted Born iterative method (DBIM) is a popular technique for reconstructing a dielectric profile from scattered fields. However, it is more challenging to reliably produce high-fidelity imagery with DBIM when the aperture formed by the sensors does not fully surround the region of interest and when noise significantly degrades the quality of the data. We propose a frequency beamforming enhancement to DBIM which builds on the previously studied spatial beamforming-enhanced DBIM by focusing across both space and frequency prior to solving for the dielectric contrast. Results for simulated data demonstrate that the frequency beamforming enhancement to DBIM results in better overall reconstructions and less sensitivity to the choice of the regularization parameter as compared to traditional DBIM and spatial beamforming-enhanced DBIM.**

I. Introduction

Electromagnetic quantitative inverse scattering (QIS) is the process of recovering both a target shape and dielectric profile from scattered electric fields. In an ideal imaging scenario, the target is fully surrounded by antennas and data is collected across multiple widely spaced frequencies, resulting in a dataset with significant spatial and frequency diversity which mitigates the ill-posed nature of the inverse problem. However, there are many practical scenarios in which antennas can only be placed across a limited aperture and data can only be collected across a narrow bandwidth due to geometry and cost constraints. This results in a reduction of spatial and frequency information which manifests itself through heightened sensitivity to noise, model error, and parameter selection.

A previously proposed spatial beamforming-enhanced (SBE) QIS method [1] focused the signals in space before carrying out a traditional DBIM [2] optimization. The beamforming in [1] introduced a spatial averaging feature that discouraged large changes between adjacent pixels, resulting in the solution being more robust to perturbations. In addition, coherent summation of the signal from target features decreased the DBIM algorithm's sensitivity to noise. We hypothesize that additional robustness could be achieved even with a small-bandwidth signal by focusing across space and frequency simultaneously, and we refer to this new approach as frequency beamforming-enhanced (FBE) DBIM.

II. Beamforming-DBIM

A. Distorted Born Iterative Method

DBIM is a quantitative and iterative reconstruction technique which uses successive linearizations of the total electric field and updates of the dyadic Green's function in order to build an approximation of the dielectric properties of a region of interest Ω. Beginning with the Born-approximated integral solution to the Helmholtz equation, we have

$$E_s(\boldsymbol{r}_T, \boldsymbol{r}_O; \omega) = \omega^2 \epsilon_0 \mu_0 \int_\Omega G_b(\boldsymbol{r}_O, \boldsymbol{r}'; \omega) E_i(\boldsymbol{r}_T, \boldsymbol{r}'; \omega) \delta\rho(\boldsymbol{r}') d\boldsymbol{r}', \tag{1}$$

where E_s, E_i are the scattered and incident electric fields, $\boldsymbol{r}_T, \boldsymbol{r}_O$ are the locations of the transmitting and receiving antennas, ω is the angular frequency, ϵ_0 and μ_0 are the background permittivity and permeability, G_b is the dyadic Green's function, $\boldsymbol{r}' \in \Omega$, and $\delta\rho$ is the dielectric contrast.

Equation (1) is discretized to form the linear system $\boldsymbol{A}(\omega)\boldsymbol{x} = \boldsymbol{b}(\omega)$, where $\boldsymbol{A}(\omega)$ represents the integral operator at frequency ω, $\boldsymbol{x}$ contains the values of $\delta\rho$ on each pixel, and $\boldsymbol{b}$ contains the scattered electric field data at frequency ω. Multiple frequencies $\omega_1, \cdots, \omega_F$ can be incorporated by stacking matrices $\boldsymbol{A}(\omega_i)$ and vectors $\boldsymbol{b}(\omega_i)$ to form the larger system denoted $\boldsymbol{A}_S\boldsymbol{x} = \boldsymbol{b}_S$. We add a Tikhonov regularization term and write the solution as

$$\boldsymbol{x} = \text{argmin}_{\tilde{\boldsymbol{x}}} \left\{ ||\boldsymbol{A}_S\tilde{\boldsymbol{x}} - \boldsymbol{b}_S||_2^2 + \alpha ||\tilde{\boldsymbol{x}}||_2^2 \right\}, \tag{2}$$

where α is a regularization parameter.

For F given matrices of bistatic scattering data $\{\boldsymbol{\mathcal{D}}(\omega_i) \mid i = 1, \ldots, F\}$ where $\boldsymbol{\mathcal{D}}_{nm}(\omega_i) = E_s(\boldsymbol{r}_{T_n}, \boldsymbol{r}_{O_m}, \omega_i)$, the DBIM algorithm proceeds by selecting a starting value of the dielectric properties ρ, computing the incident field and Green's function to form the linear system $\boldsymbol{A}_S\boldsymbol{x} = \boldsymbol{b}_S$, solving the minimization problem in equation (2), and updating the dielectric properties through $\rho = \rho + \delta\rho$. This process is repeated until a termination condition is reached.

B. DBIM with Spatial Beamforming Enhancement

In order to describe the spatial beamforming enhancement to DBIM [1], we first introduce the following notation. Let $\boldsymbol{e}_i(\boldsymbol{r}'; \omega) = [E_i(\boldsymbol{r}_1, \boldsymbol{r}'; \omega) \ \ldots \ E_i(\boldsymbol{r}_K, \boldsymbol{r}'; \omega)]^T$ and $\boldsymbol{g}_b(\boldsymbol{r}'; \omega) = [G_b(\boldsymbol{r}_1, \boldsymbol{r}'; \omega) \ \ldots \ G_b(\boldsymbol{r}_K, \boldsymbol{r}'; \omega)]^T$. Now, let $\boldsymbol{w}_{\boldsymbol{r}_f} = \boldsymbol{g}_b(\boldsymbol{r}_f)/||\boldsymbol{g}_b(\boldsymbol{r}_f)||$ be a beamforming weight vector designed to focus the transmitted and received signals at location $\boldsymbol{r}_f$. We write the linear system focused at location $\boldsymbol{r}_f$ as

$$\boldsymbol{w}_{\boldsymbol{r}_f}^H \boldsymbol{\mathcal{D}}(\omega) \boldsymbol{w}_{\boldsymbol{r}_f}^* = \omega^2 \epsilon_0 \mu_0 \int_\Omega \boldsymbol{w}_{\boldsymbol{r}_f}^H \boldsymbol{e}_i(\boldsymbol{r}'; \omega) \boldsymbol{g}_b^T(\boldsymbol{r}'; \omega) \boldsymbol{w}_{\boldsymbol{r}_f}^* \delta\rho(\boldsymbol{r}') d\boldsymbol{r}'. \tag{3}$$

We discretize the linear system in equation (3) for multiple focus locations to give the beamformed linear system

$\boldsymbol{A}_B(\omega)\boldsymbol{x} = \boldsymbol{b}_B(\omega)$. The SBE-DBIM algorithm proceeds as before with the beamformed linear system replacing the linear system $\boldsymbol{A}_S(\omega)\boldsymbol{x} = \boldsymbol{b}_S(\omega)$.

C. DBIM with Frequency Beamforming Enhancement

The conventional way to use multiple frequencies in SBE-DBIM is to stack the matrices $\boldsymbol{A}_B(\omega_1), \ldots, \boldsymbol{A}_B(\omega_F)$ and right-hand side vectors $\boldsymbol{b}_B(\omega_1), \ldots, \boldsymbol{b}_B(\omega_F)$ and solve the resulting linear system. We propose to instead add a focusing step across frequency, giving the linear system

$$\int_{\omega_1}^{\omega_F} \boldsymbol{w}_{\boldsymbol{r}_f}^H \boldsymbol{\mathcal{D}}(\omega')\boldsymbol{w}_{\boldsymbol{r}_f}^* d\omega' = \tag{4}$$
$$\int_{\omega_1}^{\omega_F} (\omega')^2 \epsilon_0\mu_0 \int_\Omega \boldsymbol{w}_{\boldsymbol{r}_f}^H \boldsymbol{e}_i(\boldsymbol{r}';\omega')\boldsymbol{g}_b^T(\boldsymbol{r}';\omega')\boldsymbol{w}_{\boldsymbol{r}_f}^* \delta\rho(\boldsymbol{r}')d\boldsymbol{r}'d\omega'.$$

In discretized form, we have

$$\left[\sum_{i=1}^{F} \boldsymbol{A}_B(\omega_i)\right]\boldsymbol{x} = \left[\sum_{i=1}^{F} \boldsymbol{b}_B(\omega_i)\right]. \tag{5}$$

This linear system replaces $\boldsymbol{A}_S(\omega)\boldsymbol{x} = \boldsymbol{b}_S(\omega)$ in the traditional multi-frequency DBIM algorithm.

III. Results

We present results for simulated data from an L-shaped dielectric target with side length 1 m and relative permittivity $\epsilon_r = 2$. Data was simulated via a 2-dimensional transverse-magnetic finite-difference time-domain simulation with antennas distributed across an array with aperture size $90°$ (see Figure 1). Signal phasors were acquired from $100 - 145$ MHz with 5 MHz frequency spacing. Gaussian noise was added to the array of bistatic scattering data in order to simulate data with SNR values of 34 dB, 20 dB, 10 dB, and 5 dB. Reconstructions were run for eight different values of α evenly spaced on a logarithmic scale from 10^{-6} to 10 for each of these four different noisy data sets. For both SBE-DBIM and FBE-DBIM, 121 beamforming foci were distributed in the domain with spacing 0.7 m in each direction.

Figure 2 displays reconstructions for traditional DBIM, SBE-DBIM, and FBE-DBIM for four different values of α at SNR 20 dB. The left side of Figure 3 shows the values of the L^2 error of the difference between the reconstructed relative permittivity and true relative permittivity against the regularization parameter, while the right side of Figure 3 displays the L^2 error of the optimal reconstruction at each SNR value, selected using a heuristic similar to the L-curve method [3].

IV. Conclusions

The results presented for the L-shaped scatterer in Figures 2 and 3 show that the FBE-DBIM algorithm outperformed both standard DBIM and SBE-DBIM for the scenario described in Section III. In particular, the FBE-DBIM algorithm displays less sensitivity to the choice of the regularization parameter α. In addition, as the SNR degrades to 20 dB and below, the frequency beamforming enhancement produces the optimal reconstruction both qualitatively and with respect to the L^2 error.

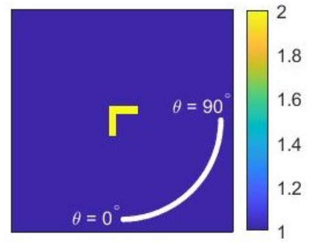

Fig. 1: L-shaped target with relative permittivity $\epsilon_r = 2$ and location of the $90°$ aperture used to collect data.

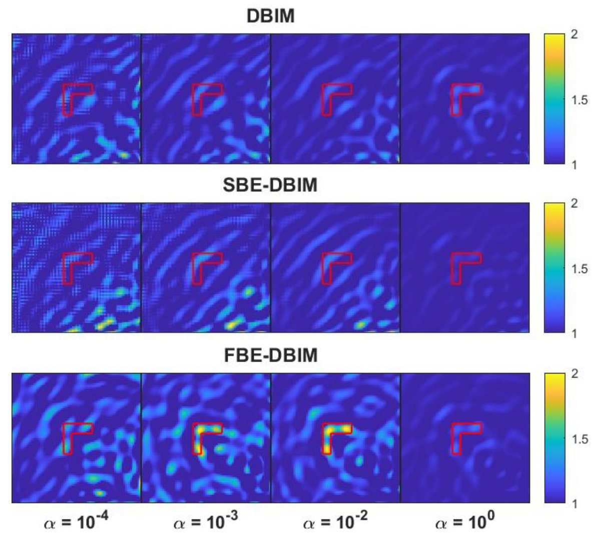

Fig. 2: Reconstructed relative permittivity of L-shaped target for four values of α with an SNR of 20 dB.

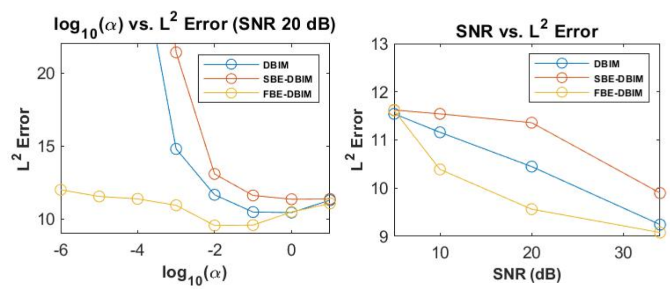

Fig. 3: Plots of the L^2 error in the reconstructed relative permittivity against α (for an SNR of 20 dB) and the L^2 error against SNR.

Acknowledgement

This work was funded by the Office of Naval Research via the NRL 6.2 Base Program.

References

[1] M. Burfeindt, J. Shea, B. Van Veen, and S. Hagness, "Beamforming-Enhanced Inverse Scattering for Microwave Breast Imaging", *IEEE Trans Antennas Propag.*, Oct. 2014.

[2] W. C. Chew and Y. M. Wang, "Reconstruction of two-dimensional permittivity distribution using the distorted Born iterative method", *IEEE Transactions on Medical Imaging*, vol. 9, no. 2, pp. 218-225, June 1990.

[3] P.C. Hansen and D.P. O'Leary, "The use of the L-curve in the regularization of discrete ill-posed problems", *SIAM journal on scientific computing*, vol. 14, no. 6, pp. 1487-1503, 1993.